



Some aspects of deep-bed filtration dynamics in QMRA for drinking water

Vegard Nilsen

Norwegian University of Life Sciences, Faculty of Science and Technology, P.O.Box 5003, N-1432, Ås, Norway



ARTICLE INFO

Article history:

Received 9 September 2019

Received in revised form

17 November 2019

Accepted 1 December 2019

Available online 6 December 2019

Keywords:

microbial risk

QMRA

Drinking water

Filtration

Dynamics

ABSTRACT

Unlike most unit processes in drinking water treatment, the performance of deep-bed filtration processes vary *systematically* on short time-scales; the particle removal capacity changes with time since the previous backwash, even when the influent water quality is stable. For microorganisms, the removal efficiency may vary by orders of magnitude. In this note, the potential impact of such dynamics on microbial risk estimates is studied, using representative experimental filtration data for viruses and bacteria in conjunction with single-hit dose-response models for microbial infection.

Assuming that filtration is the only source of variation in pathogen concentrations on the time-scale of a single filter cycle, it is concluded that such variations are unlikely to substantially affect risk estimates, except possibly in an outbreak situation with extremely high pathogen concentrations; it is generally sufficient to know the *mean* pathogen concentrations. Future studies should include concurrent variation in the performance of other unit processes and raw water pathogen concentrations. Experimental work should focus on capturing the variation in filtration performance in order to correctly estimate *mean* removal rates.

© 2019 The Author. Published by Elsevier Ltd. This is an open access article under the CC BY license (<http://creativecommons.org/licenses/by/4.0/>).

1. Introduction

A treatment train involving some combination of coagulation, flocculation, sedimentation and *deep-bed filtration* is common in water treatment plants throughout the world. While designed for removing particles and/or natural organic matter (NOM) in general, coagulation-filtration processes also account for a significant portion of the overall microorganism removal, including pathogens (Hijnen and Medema, 2010).

There are several sources of variation in the microbial removal efficiency of filtration processes. Variation among plants exists due to differences in design, raw water quality and operational practices. There may be slow variations in time, e.g. because of a changing raw water composition throughout the year (Westrell et al., 2006), or there may be rapid and more random variations as a result of raw water contamination events (Signor et al., 2005; Åström et al., 2013) or failures in the treatment processes (Hijnen and Medema, 2010; Huck et al., 2002; Emelko et al., 2003).

However, superimposed on the variations already mentioned, there may be *systematic* short-term variations in removal efficiency

originating from the inherently dynamic character of the deep-bed filtration process during normal operation, even if influent water quality characteristics remain constant. Typically, as measured by filter effluent turbidity, there is an initial period of improvement in performance as the filter begins to collect particles (the ripening period), followed by a period of relatively stable performance until the performance eventually deteriorates (the breakthrough phase when the particle collection capacity is exhausted). The filter must then be taken out of service to be backwashed so that the particle collection capacity can be restored to its initial state (i.e. the process is discontinuous and essentially periodic). These dynamic characteristics distinguish the filtration process from other typical unit processes in conventional treatment (sedimentation, flotation, chlorination, UV irradiation), that are comparatively stable and uninterrupted during normal operation and when subjected to a constant influent water quality.

Turbidity removal dynamics during filtration is not entirely representative of microbial filtration dynamics, though, since turbidity measurements lump the contribution of all particle types into a single parameter. Several studies have shown that the ripening and breakthrough behavior is dependent on – among several physico-chemical properties – particle size (Clark et al., 1992; Kim and Lawler, 2008; Moran et al., 1993), with smaller

E-mail address: vegard.nilsen@nmbu.no.

particles typically taking longer to both ripen and break through as compared to larger particles. Some studies have shown a marked reduction in microorganism removal early and late in the filter cycle (Robeck et al., 1962; Harrington et al., 2003; Emelko et al., 2003; Templeton et al., 2007). Still, studies that aim to characterize microbial removal rates of filtration processes are usually focused on “typical” removal rates, i.e. removal rates during periods of stable effluent turbidity, often employing sampling regimes that are unable to capture the full variation in treatment efficiency throughout the filter cycle.

Recently, we undertook a pilot-scale dual-media contact-filtration study in an attempt to generate a high-resolution sample of such microbial filtration dynamics during an entire filter cycle (Nilsen et al., 2019). The instantaneous removal efficiency of model viruses and bacteria varied by a factor of about 50 and 200, respectively, during the period when effluent turbidity was less than 0.1 NTU, indicating that the dynamic character of filtration processes should not a priori be overlooked in risk assessment.

In *quantitative microbial risk assessment* (QMRA; Haas et al., 2014), variations in removal rates may be modeled by fitting appropriate probability distributions to data from filter influent and effluent samples (Teunis et al., 1999, 2009; Smeets et al., 2008). Such fitted distributions may be used together with data on raw water quality and other treatment processes to estimate the exposure of water consumers to pathogens. Data on exposure is subsequently used as input to dose-response models (Haas, 1983; Nilsen and Wyller, 2016a) for estimating microbial risks associated with drinking water consumption.

The effect of short-term systematic variations in microbial filtration efficiency, that are present during normal operation, has received comparatively less attention in the microbial risk literature. In this note, we will use our example high-resolution dataset (Nilsen et al., 2019) to

- compute probability distributions for microorganism removal in a single filter during one filter cycle
- evaluate the effect on risk estimates when assuming that concentration variations from filtration persist until a point of consumption and there are no other sources of variation
- discuss the overall relevance of filtration dynamics for QMRA

In most water supply systems, variation in filter effluent concentrations will be subject to smoothing by e.g. storage tanks and mixing of effluents from filters operating in parallel. Thus, the assumption that variations in concentration actually reach the consumer is a limiting case – I will return to this issue in the discussion.

2. Data and methods

2.1. Example data

The filtration experiment that generated the example data is reported in full elsewhere (Nilsen et al., 2019). The experimental setup was representative of Norwegian filtration practice (Ødegaard et al., 2010). Three model microorganisms were used; bacteriophage MS2 (icosahedral, 27 nm), bacteriophage *Salmonella* Typhimurium 28B (icosahedral, 60 nm) and indicator bacterium *E.coli* (rod-shaped, approx. 1 μm \times 3 μm). These were chosen mainly because more data on virus removal has been sought in Norway and it was relatively simple to include *E.coli* as an additional organism. The approach velocity was constant. Fig. 1 shows the logarithm of π , the instantaneous probability of passage, for each organism as a function of elapsed time in the filter cycle, t . More precisely,

$$\pi(t) = \frac{C_{\text{out}}(t)}{C_{\text{in}}(t)} \quad (1)$$

Here, C_{out} and C_{in} are, respectively, the effluent and influent concentrations (as number of microorganisms/unit volume) of the filter. The commonly used log-removal rate is simply $-\log_{10}(\pi)$. Note that in formulating (1), we ignored the travel time between filter inlet and outlet, which is short compared to the time-scale of changes in π . The strict interpretation of π as the probability of passage of a single organism requires π to be independent of both influent and attached microorganism concentrations; see Nilsen et al. (2019) for further details.

The data shows that bacteria were generally removed better than viruses, and the results are also consistent with expectations based on the size-difference between the organisms: ripening for bacteria occurred more rapidly than for viruses, and bacteria broke through before viruses. We define breakthrough here as the onset of persistently increasing passage. Both organisms broke through before turbidity, though, confirming that there are limitations in using turbidity as a surrogate for microorganism removal. It is noted that the breakthrough of viruses is rather abrupt compared to the more gradual breakthrough of bacteria. Computations reported in this note were performed directly on the experimental data, interpolating linearly between data points to construct a continuous function $\pi(t)$.

The most important implication for risk assessment related to filtration dynamics is probably the challenge it poses to correctly estimating *mean* removal efficiencies over a full filter cycle. This part of the problem was studied in Nilsen et al. (2019), where it was shown that true mean removal efficiencies may deviate from mid-cycle instantaneous removal efficiencies by more than one \log_{10} unit. The present note explores further the impact of filtration dynamics itself for QMRA, given that the mean removal is already known.

2.2. Probability distribution for Π from $\pi(t)$

Filtration dynamics may induce *systematic* variations, but these must *be treated as random* from a consumer’s point of view, since a consumer essentially samples a random volume from the water supply. For use in risk assessment applications, it is of interest to derive a proper probability distribution for a random variable Π representing the observed variation in microbial removal efficiency during filtration.

Some precision is needed in describing this mathematically. In general, a consumer is assumed to sample uniformly from the total volume produced (flow proportional sampling) which, if the flow rate $q(t)$ is non-constant, is *not equivalent* to sampling uniformly in time. The flow rate was constant in our filtration experiment, but that is not always how filters are operated. The accumulated volume of water $v(t)$ produced in the time interval $[0, t]$ is given by

$$v(t) = \int_0^t q(\tau) \, d\tau \Leftrightarrow \frac{dv}{dt} = q(t) \quad (2)$$

Since $q(t)$ is positive, $v(t)$ is one-to-one and may be inverted to give a function $t(v)$. When $\pi(t)$ is given, we may therefore express π as a function of v , $\pi[t(v)]$, and use the theory of functions of random variables (Appendix A) to obtain the probability distribution for the random variable $\Pi[t(V)]$ when V is a uniformly distributed random variable on $[0, v]$. It is assumed here that the sample volume is so small that we may treat $\pi(t)$ as constant during the time interval needed to sample a small volume.

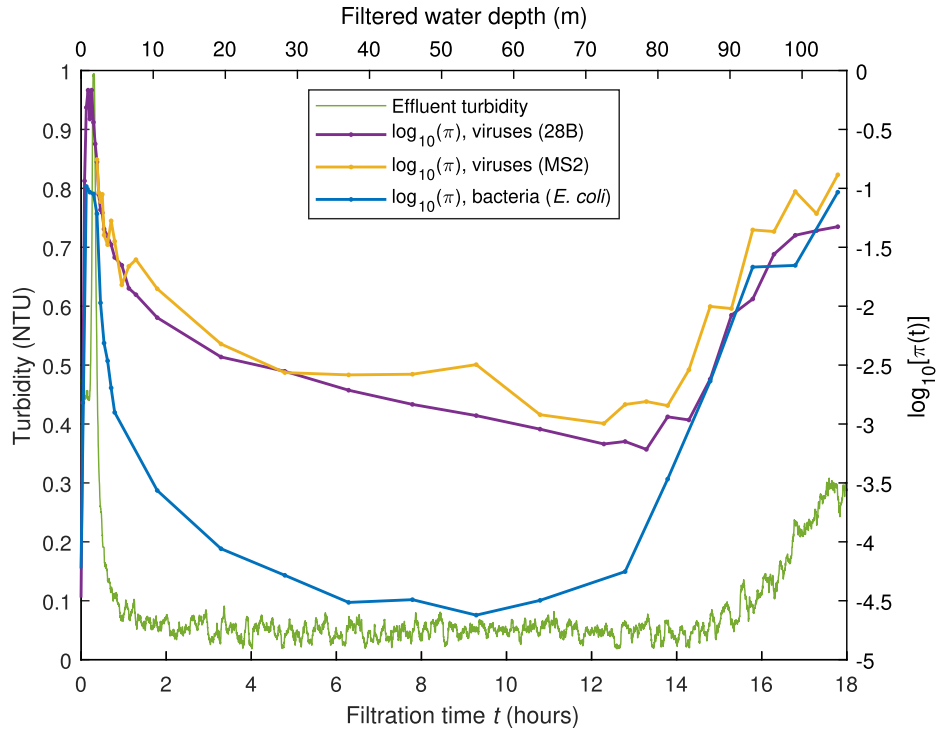


Fig. 1. Data from the filtration experiment described in Section 2.1. After backwash, the filter was run briefly with raw water to displace the backwash water and $t = 0$ corresponds to the first arrival of coagulated water at the filter surface. The theoretical clean bed retention time in the filter was approx. 7 min.

2.3. The effect of variation in π on risk estimates

In QMRA, data on pathogen concentrations (with variations) are used as input to dose-response models to estimate the probability of infection from drinking water. Since dose-response models are *non-linear* in the dose variable, knowing the mean dose is generally insufficient; the full dose distribution is required for a precise calculation of risk. It is therefore of interest to study the effect of variations in π from filtration (as it affects the dose distribution) on risk estimates from dose-response models.

The *single-hit* dose-response framework (Haas, 1983; Nilsen and Wyller, 2016a), of which the exponential and beta-Poisson models are examples, has served as the de facto standard modeling approach for drinking water. A generic formulation is given by

$$P_I = 1 - \int_0^1 G_X(1-r)f_R(r) dr \quad (3)$$

where P_I is the probability of infection, G_X is the probability generating function (pgf) of the dose variable X (number of organisms ingested), and f_R is the probability density function (pdf) of the so-called single-hit probability R , which may vary between hosts, but variation between individual pathogens is integrated out (Fazekas de St Groth and Moran, 1955; Haas, 2002; Schmidt et al., 2013; Nilsen and Wyller, 2016b).

In the simplest case of constant pathogen concentration, the dose X is taken to be Poisson distributed with mean $\lambda = cv_s$, where v_s is the sample volume. If concentrations vary, X is typically constructed as a mixed Poisson distribution with random Poisson parameter $\Lambda = Cv_s$. Furthermore, if one assumes that, on the time scale of a filter cycle, the only source of variation in concentrations is filtration performance, one may write $\Lambda = k\Pi$, where k is a constant with units of dose. For such mixed Poisson dose

distributions, Equation (3) can be written

$$P_I = 1 - \int_0^1 M_\Lambda(-r)f_R(r) dr = 1 - \int_0^1 M_\Pi(-kr)f_R(r) dr \quad (4)$$

where M is a moment-generating function (mgf) and the latter equality applies when $\Lambda = k\Pi$. The evaluation of (4) using experimental data is treated in Appendix A.

In order to gain an understanding of the potential effects of filtration dynamics on risk estimates, the following risk ratio may be evaluated where, for simplicity, we have assumed a constant single-hit probability r :

$$\frac{P_{I,\text{dist}}}{P_{I,\text{mean}}} = \frac{1 - M_\Pi(-rk)}{1 - e^{-rkE(\Pi)}} \quad (5)$$

The numerator is the single-exposure risk computed with the full distribution of $\Lambda = k\Pi$. The denominator is the single-exposure risk computed with the exponential model with mean dose $E(\Lambda) = kE(\Pi)$, i.e. the mean dose is the same in both cases. The risk computed with a mixed Poisson dose distribution is always less than the risk computed with a Poisson distribution with the same mean (Nilsen and Wyller, 2016b, Proposition 2).

The treatment above assumed that X is the mixed Poisson dose distribution resulting from a single exposure. The risk resulting from n doses, independent and identically distributed as X , is given by (Nilsen and Wyller, 2016a):

$$P_I = 1 - \int_0^1 [M_\Lambda(-r)]^n f_R(r) dr \quad (6)$$

3. Analysis and results

3.1. Probability distribution for Π from $\pi(t)$

For given start and end times of the production period (end of filter-to-waste and initiation of backwashing, respectively), the probability distribution of Π may be derived from $\pi(t)$ using the relationships described in Section 2.2 and Appendix A. This has been done with our example data to produce Fig. 2, which shows cumulative distribution functions (cdf) for three different production periods, for viruses and bacteria. For viruses, we have also included a comparison with a cdf derived by Teunis et al. (2009). They used data on F-specific coliphages from two plants in the Netherlands to estimate a beta distribution for the removal during coagulation-filtration, assuming paired influent and effluent samples and gamma-distributed influent concentrations.

As seen in Fig. 2, the distribution for bacteria is generally

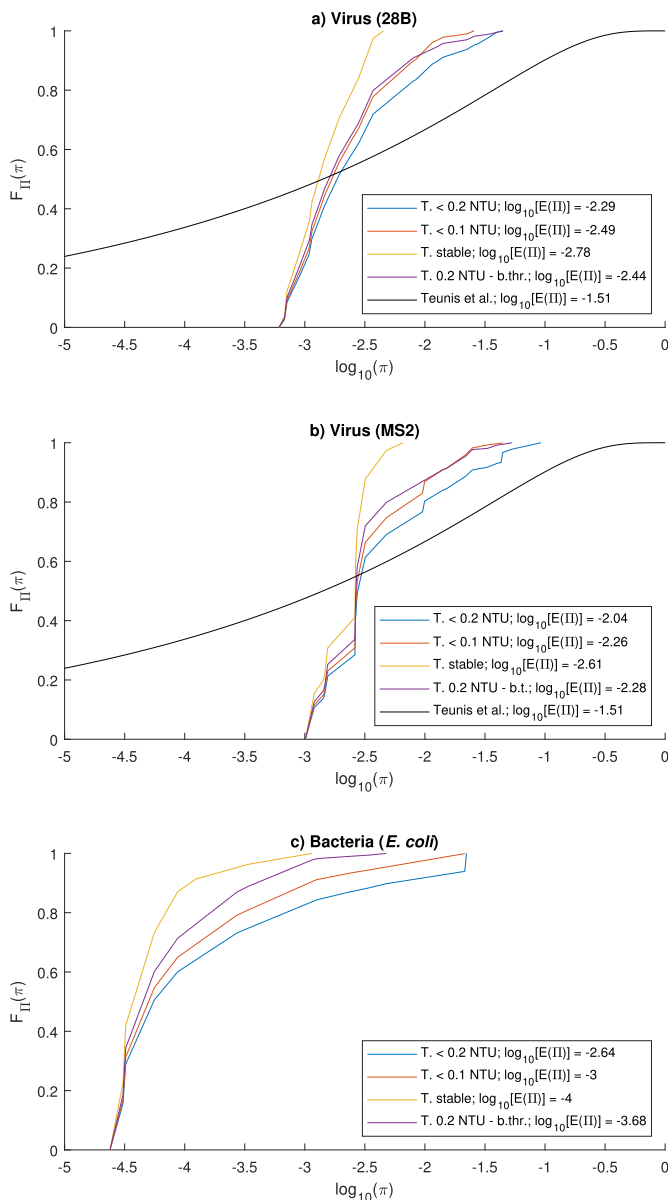


Fig. 2. Cumulative probability distributions for passage probability Π derived from $\pi(t)$ of the example data in Fig. 1, using the methods outlined in Section 2.2 and Appendix A.

displaced to the left compared to the viruses, reflecting its better removal, also seen in Fig. 1. The near vertical parts of the distributions stem from the near horizontal parts of the curves in Fig. 1. Restricting the length of the production period displaces probability mass to the left. It is clear that the estimated beta cdf of Teunis et al. (2009) is vastly more spread out than our empirical cdfs from a single filter run, although the median values of Π are close to each other. However, the data that went into estimating the beta cdf was of a very different nature (high volume sampling with a subsequent concentration step, two different plants, only 17 samples in total) than our experimental data, and there was no detailed information on process characteristics or consideration of filtration dynamics. The difference is nevertheless consistent with the observation that highly variable virus removal efficiencies for filtration are reported in the literature (Nilsen et al., 2019, Supplementary data). Such cdfs as generated here from our filtration experiment, or perhaps some smoother versions of them, may potentially be used as input for Monte-Carlo simulations in detailed risk assessment models.

3.2. The effect of variation in π on risk estimates

Plots of the risk ratio in equation (5) are shown in Fig. 3a and b for viruses (28B) and bacteria, respectively. They show the influence of 1) varying the production period by restricting the effluent turbidity and 2) the parameter rk through its effect on the exponential model risk (horizontal axes). Also shown in Fig. 3a is the risk ratio computed with the beta distributed π from Teunis et al. (2009), for which the mgf in equation (5) becomes ${}_1F_1(\alpha, \alpha + \beta, -rk)$, where ${}_1F_1$ is Kummer's confluent hypergeometric function and α and β are parameters of the beta distribution.

As dictated by theory, Fig. 3a and b shows that the ratio in equation (5) is less than 1. We see that the effect of variation in π on risk estimates tends to be more pronounced when lesser restrictions are placed on effluent turbidity. It should be noted that under normal operating conditions, when the single-exposure risk is typically less than 10^{-6} , variation in π alone appears to have negligible influence on risk estimates. This applies also when using the very wide π -distribution from Teunis et al. (2009). These observations are related to the well-known fact that single-hit models become approximately linear at low doses. Variation in π only seems to become important under severe outbreak conditions, when the single-exposure risk is higher than 0.01 and somewhat away from 1. For Fig. 3b for bacteria, we find the same tendencies as for viruses, but slightly more pronounced due to the characteristics of the π -variation.

As an example of an equivalent calculation using a model with a variable single-hit probability r , Fig. 4 shows the following risk ratio for norovirus:

$$\frac{P_{I,\text{dist}}}{P_{I,\text{mean}}} = \frac{1 - \int_0^1 {}_1F_1(\alpha, \alpha + \beta, -k\pi) f_{\Pi}(\pi) d\pi}{1 - {}_1F_1(\alpha, \alpha + \beta, -kE(\Pi))} \quad (7)$$

The denominator is the risk computed using the ordinary exact beta-Poisson model and the numerator is the risk computed with a variable π . The norovirus parameters $\alpha = 0.040$ and $\beta = 0.055$ are taken from Teunis et al. (2008) and gives a very dispersed distribution. The results are qualitatively similar to the results in Fig. 3.¹

These figures apply to the single-exposure case. For the multiple exposure case (n exposures), we have the corresponding ratio

¹ No results are shown for the π -distribution from Teunis et al. (2009) as the required numerical integration was problematic in MATLAB.

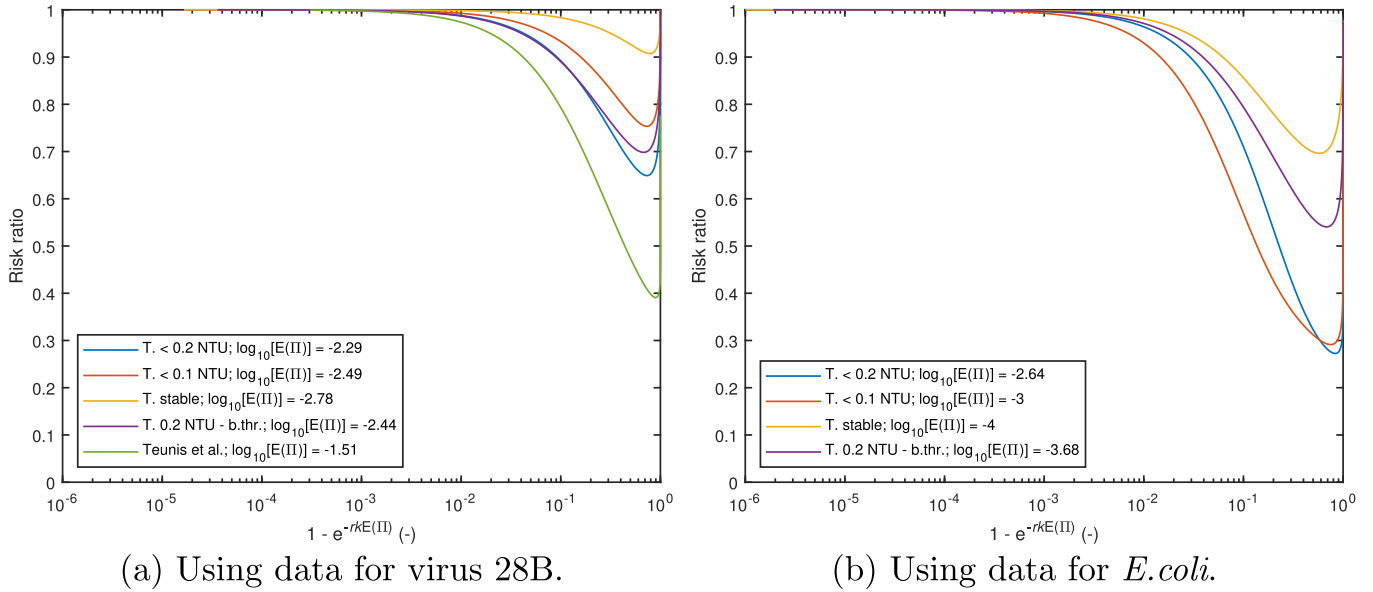


Fig. 3. Plots of the risk ratio in equation (5).

$$\frac{P_{I,nd}}{P_{I,d}} = \frac{1 - [M_{II}(-rk)]^n}{1 - e^{-nrkE(II)}} \quad (8)$$

It is readily shown that this ratio *increases* towards 1 as n increases since $M_{II}(-rk) > e^{-rkE(II)}$. Thus, the effect of variations in π only tend to become less important as the number of exposures increases.

4. Discussion

Here we will first address some limitations associated with our example dataset and computational model before briefly discussing the overall relevance of filtration dynamics for risk assessment.

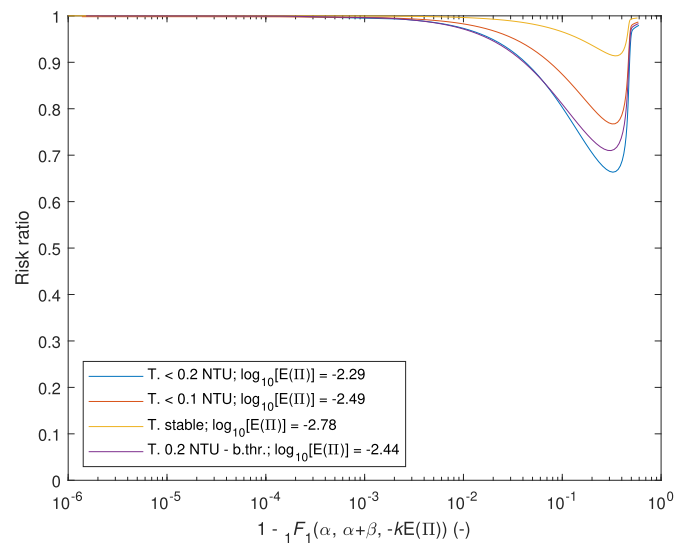


Fig. 4. Plot of the risk ratio in equation (7) using removal data for viruses and dose-response parameters for norovirus (Teunis et al., 2008).

4.1. Limitations of the example data and computations

4.1.1. Example data

The example dataset represents the most highly resolved characterization of microbial removal in a single deep-bed filter cycle that we are aware of, at least for viruses. The observed variation in performance throughout the filter cycle was substantial, qualitatively as expected based on virus and bacteria relative sizes (Clark et al., 1992; Moran et al., 1993), and is believed to represent real-world phenomena occurring in water treatment plants. Still, the data has been obtained under a single set of experimental conditions, corresponding to common filtration practice in the Nordic countries, and is not necessarily representative of filtration processes that operate under different conditions. Specifically, one may wish to conduct high-resolution characterizations using pre-sedimentation, dedicated flocculation steps, different filter rates, declining-rate filtration, different filter materials, different coagulants, filter aids/polymers and more particle-rich raw water. Furthermore, other surrogate organisms for pathogens should be tested in future high-resolution characterizations.

4.1.2. Computations

Some of the limitations of the computational model that could be investigated in future research efforts, include:

- *Unaccounted-for variation.* In our computations, the only varying quantity on the time scale of a filter cycle was the filtration passage probability. In reality, there may be random variations in raw water concentrations and the performance of other unit processes (e.g. because of operational failure) that are relevant on similar time scales. If such variations are present and can be taken as independent of the variation in filtration performance, it will lead to *increased* variation in the dose distributions.
- *Filters in parallel.* Our example computations relied on the passage probabilities through a *single filter*. In a real water treatment plant there will be a gallery of filters operating in parallel, with the effluents from each filter being mixed at some downstream junction. The filters will be at different stages in their filter cycles and the mixing of effluents will have a certain

smoothing effect on the dose distribution. A rudimentary model of such effects may be found in Nilsen (2016). Another effect to consider is the *hydraulic step*: when one filter is taken out of service for backwashing, the filtration rate through the remaining filters may increase and may affect the removal efficiency.

- *The effect of distribution systems.* The relevance of filtration dynamics depends on the extent to which the distribution system disperses pathogens and smooths out the variations that exist at the treatment plant. This will likely depend on the layout of the pipe network and storage tanks in the system, the distribution of water demands and the location of each individual consumer within the network.
- *Dose response models.* Single-hit dose-response models are routinely used for drinking water risk assessment and have been shown to fit data well for medium-to-high doses. It is, however, a remaining scientific challenge to verify their applicability for low doses, so that extrapolations beyond the range of observations is typically necessary for drinking water studies. If the true dose-response model is non-linear even for low doses, this will affect the results of modeling efforts where variation in doses is accounted for. Furthermore, we considered only one case of variable single-hit probability r in our examples. Such models are “flatter” than their constant- r counterparts (Nilsen and Wyller, 2016a, Proposition 1), but qualitatively similar; we do not expect the main conclusions to change with such models and further calculations (not shown) using equation (7) with combinations of α and β in the range 0.5–5 support this.

4.2. Filtration dynamics and risk assessment

The existence of filtration dynamics poses two main challenges to microbial risk assessment: Correctly estimating the mean passage probability and hence mean pathogen concentrations and doses, and the possibility that variations around the mean concentration may significantly affect risk estimates.

The plots in Figs. 3 and 4 indicate that concentration variations around the mean exert all but negligible influence in our risk model with the example dataset, except possibly in a situation where pathogen concentrations approach levels associated with extreme risk and attack rates. This applies even when using the π -distribution from Teunis et al. (2009), which is significantly more spread out than our experimental π -distributions. We stress that this result applies to a situation where we ignore other sources of variation in the dose distribution on the time scale of a filter cycle. The conclusion seems robust as several assumptions were made in this study that will overexaggerate the variation in the dose distribution, including ignoring effects of parallel filters, ignoring mixing in the distribution system and ignoring the effect of multiple exposures.

Correctly estimating and minimizing the mean passage probability of deep-bed filters therefore seems to be the more important aspect of filtration dynamics for risk assessment and management. This aspect was studied in detail in Nilsen et al. (2019). For long-term risk assessments, it may still be useful to include empirical distributions such as those given in Fig. 2 into Monte Carlo simulations of risk. The distributions in Fig. 2 are available from the author upon request.

5. Conclusions

In this note, we have studied the effect of short-term deep-bed filtration dynamics on microbial risk estimates, using high-resolution data on filtration performance that is believed to be representative of real world effects under the given conditions,

together with a simplified conceptual model. Under the assumption that filtration performance is the only variable quantity on the time-scale of a single filter cycle, it was shown that concentration variations induced by filtration are unlikely to affect risk estimates when compared with a model that uses an equivalent mean concentration, except possibly in an outbreak situation with extremely high pathogen concentrations. Future studies should probe this result further by studying the effect of concurrent variation in filtration performance and other unit processes, as well as raw water concentrations. Until further studies along the suggestions made above can be carried out, the main consequence for QMRA of systematic, short-term dynamic effects in microbial filtration performance, is to motivate filtration experiments to correctly estimate *mean* passage probabilities under a wider range of conditions.

Declaration of competing interest

The authors declare that they have no known competing financial interests or personal relationships that could have appeared to influence the work reported in this paper.

Acknowledgements

Discussions with Profs. Arve Heistad and John Wyller were very helpful in the preparation of this manuscript.

Appendix A. The transformation-rule for functions of random variables

Assume that we have a random variable V with associated probability density function $f_V(v)$ and a differentiable function $g: \mathbb{R} \rightarrow \mathbb{R}$ that induces a new random variable $\Pi = g(V)$. Assume that the domain of the function g may be partitioned into n intervals such that the function g is monotonic on each interval. Denote the restriction of g to interval i by g_i . Then the probability density of Π is given by

$$f_{\Pi}(\pi) = \sum_{i=1}^n f_V \left[g_i^{-1}(\pi) \right] \left| \frac{dg_i^{-1}(\pi)}{d\pi} \right| \quad (\text{A.1})$$

It is assumed here that $\Pr[g(V) = 0] = 0$. If that is not the case, the above rule can be generalized and the density $f_{\Pi}(\pi)$ becomes a mixed discrete-continuous probability distribution, i.e. it has some point masses of probability.

When V is uniformly distributed on $[v_1, v_2]$, the rule simplifies to

$$f_{\Pi}(\pi) = \frac{1}{v_2 - v_1} \sum_{i=1}^n \left| \frac{dg_i^{-1}(\pi)}{d\pi} \right| \quad (\text{A.2})$$

This expression may be evaluated numerically from the example experimental data in Fig. 1, from which the associated cumulative distributions shown in Fig. 2 can be computed. In parentheses, it is noted that this procedure closely parallels the construction of flow duration curves in hydrology.

Now, introduce another function $h: \mathbb{R} \rightarrow [0, 1]$ that maps π to $h(\pi)$. For the expected value $E[h(\Pi)]$, we have according to (A.2) and a change of variables

$$E[h(\Pi)] = \int_{\Pi} h(\pi) f_{\Pi}(\pi) d\pi = \frac{1}{v_2 - v_1} \int_{v_1}^{v_2} h[g(v)] dv \quad (\text{A.3})$$

Thus, expectations over Π are equivalent to simple averages over V when V is uniformly distributed, which is, of course, in agreement with intuition.

As stated in equation (4), when the dose variable $\Lambda = k\Pi$, the single-hit dose-response model is constructed with the moment generating function (mgf) of Π evaluated at $-rk$. The mgf of Π is an expectation value on the form given in (A.3), with $h(\Pi) = e^{z\Pi}$. When $\Pi = g(V)$ with V uniformly distributed, the mgf of Π may be computed as

$$M_{\Pi}(z) = E(e^{z\Pi}) = \frac{1}{v_2 - v_1} \int_{v_1}^{v_2} e^{zg(v)} dv \quad (\text{A.4})$$

This quantity can be straightforwardly evaluated numerically from the example experimental data in Fig. 1.

References

- Åström, J., Pettersson, T.J.R., Reischer, G.H., Hermansson, M., 2013. Short-term microbial release during rain events from on-site sewers and cattle in a surface water source. *J. Water Health* 11, 430–442. <https://doi.org/10.2166/wh.2013.226>.
- Clark, S.C., Lawler, D.F., Cushing, R.S., 1992. Contact filtration: particle size and ripening. *J. Am. Water Work. Assoc.* 84, 61–71.
- Emelko, M.B., Huck, P.M., Douglas, I.P., 2003. Cryptosporidium and microsphere removal during late in-cycle filtration. *J. Am. Water Work. Assoc.* 95, 173–182.
- Fazekas de St Groth, S., Moran, P.A.P., 1955. Appendix: a mathematical model of virus-cell interaction. *J. Hyg.* 53, 291–296. <https://doi.org/10.1017/S0022172400000760>.
- Haas, C.N., 1983. Estimation of risk due to low doses of microorganisms: a comparison of alternative methodologies. *Am. J. Epidemiol.* 118, 573–582.
- Haas, C.N., 2002. Conditional dose-response relationships for microorganisms: development and application. *Risk Anal.* 22, 455–463. <https://doi.org/10.1111/0272-4332.00035>.
- Haas, C.N., Rose, J.B., Gerba, C.P., 2014. *Quantitative Microbial Risk Assessment*, 2 ed. John Wiley & Sons, Inc, Hoboken, New Jersey. <https://doi.org/10.1002/9781118910030>.
- Harrington, G.W., Xagorarakis, I., Assavasilavasukul, P., Standridge, J.H., 2003. Effect of filtration conditions on removal of emerging pathogens. *J. Am. Water Work. Assoc.* 95, 95–104.
- Hijnen, W.A.M., Medema, G.J., 2010. *Elimination of Microorganisms by Water Treatment Processes*. IWA Publishing. <https://doi.org/10.2166/9781780401584>.
- Huck, P.M., Coffey, B.M., Emelko, M.B., Maurizio, D.D., Slawson, R.M., Anderson, W.B., van den Oever, J., Douglas, I.P., O'Melia, C.R., 2002. Effects of filter operation on *Cryptosporidium* removal. *J. Am. Water Work. Assoc.* 94, 97–111.
- Kim, J., Lawler, D.F., 2008. Influence of particle characteristics on filter ripening. *Separ. Sci. Technol.* 43, 1583–1594. <https://doi.org/10.1080/01496390801974688>.
- Moran, D.C., Moran, M.C., Cushing, R.S., Lawler, D.F., 1993. Particle behavior in deep-bed filtration: Part 1—ripening and breakthrough. *J. Am. Water Work. Assoc.* 85, 69–81.
- Nilsen, V., 2016. *Quantitative Microbial Risk Assessment for Drinking Water: Dose-Response Theory and Virus Filtration Dynamics*. Ph.D. thesis. Norwegian University of Life Sciences, Ås, Norway.
- Nilsen, V., Christensen, E., Myrmed, M., Heistad, A., 2019. Spatio-temporal dynamics of virus and bacteria removal in dual-media contact-filtration for drinking water. *Water Res.* 156, 9–22.
- Nilsen, V., Wyller, J., 2016a. Qmra for drinking water: 1. revisiting the mathematical structure of single-hit dose-response models. *Risk Anal.* 36, 145–162.
- Nilsen, V., Wyller, J., 2016b. Qmra for drinking water: 2. the effect of pathogen clustering in single-hit dose-response models. *Risk Anal.* 36, 163–181.
- Ødegaard, H., Østerhus, S., Melin, E., Eikebrokk, B., 2010. NOM removal technologies – Norwegian experiences. *Drink. Water Eng. Sci.* 3, 1–9. <https://doi.org/10.5194/dwes-3-1-2010>.
- Robeck, G.G., Clark, N.A., Dostal, K.A., 1962. Effectiveness of water treatment processes in virus removal. *J. Am. Water Work. Assoc.* 54, 1275–1292.
- Schmidt, P.J., Pintar, K.D.M., Fazil, A.M., Topp, E., 2013. Harnessing the theoretical foundations of the exponential and beta-Poisson dose-response models to quantify parameter uncertainty using Markov chain Monte Carlo. *Risk Anal.* 33, 1677–1693. <https://doi.org/10.1111/risa.12006>.
- Signor, R.S., Roser, D.J., Ashbolt, N.J., Ball, J.E., 2005. Quantifying the impact of runoff events on microbiological contaminant concentrations entering surface drinking source waters. *J. Water Health* 3, 453–468. <https://doi.org/10.2166/wh.2005.052>.
- Smeets, P.W.M.H., Dullemond, Y.J., Van Gelder, P.H.A.J.M., Van Dijk, J.C., Medema, G.J., 2008. Improved methods for modelling drinking water treatment in quantitative microbial risk assessment; A case study of *Campylobacter* reduction by filtration and ozonation. *J. Water Health* 6, 301–314. <https://doi.org/10.2166/wh.2008.066>.
- Templeton, M.R., Andrews, R.C., Hofmann, R., 2007. Removal of particle-associated bacteriophages by dual-media filtration at different filter cycle stages and impacts on subsequent UV disinfection. *Water Res.* 41, 2393–2406. <https://doi.org/10.1016/j.watres.2007.02.047>.
- Teunis, P.F.M., Evers, E.G., Slob, W., 1999. Analysis of variable fractions resulting from microbial counts. *Quant. Microbiol.* 1, 63–88. <https://doi.org/10.1023/A:1010028411716>.
- Teunis, P.F.M., Moe, C.L., Liu, P., Miller, S.E., Lindesmith, L., Baric, R.S., Le Pendu, J., Calderon, R.L., 2008. Norwalk virus: how infectious is it? *J. Med. Virol.* 80, 1468–1476. <https://doi.org/10.1002/jmv.21237>.
- Teunis, P.F.M., Rutjes, S.A., Westrell, T., de Roda Husman, A.M., 2009. Characterization of drinking water treatment for virus risk assessment. *Water Res.* 43, 395–404. <https://doi.org/10.1016/j.watres.2008.10.049>.
- Westrell, T., Teunis, P., van den Berg, H., Lodder, W., Ketelaars, H., Stenström, T.A., de Roda Husman, A.M., 2006. Short- and long-term variations of norovirus concentrations in the Meuse river during a 2-year study period. *Water Res.* 40, 2613–2620. <https://doi.org/10.1016/j.watres.2006.05.019>.